MULTIROBOT SYSTEMS

Scalable robot collective resilience by sharing resources

Kevin Holdcroft[1,2], Anastasia Bolotnikova[1,3], Antoni Jubés Monforte[1], Jamie Paik[1]*

No system is immune to failure. The compromise between reducing failures and improving adaptability is a recurring problem in robotics. Modular robots exemplify this tradeoff, because the number of modules dictates both the possible functions and the odds of failure. We reverse this trend, improving reliability with an increased number of modules by exploiting redundant resources and sharing them locally. We present a unified methodology for local resource sharing; local power sharing balances energy distribution, hybrid communication spreads messages, and local sensor fusion propagates full system state estimate information among the robot collective. We present the experimental results of our methodology applied to a modular robot, Mori3. Despite one module being deprived of its own resources in terms of power, sensing, and communication, the robot collective can successfully perform a locomotion mission in a challenging environment, thanks to neighboring modules supporting each other via our proposed resource-sharing methodology.

INTRODUCTION

Designing a system resilient to failure is a long-standing and still pertinent problem in robotics (*1*, *2*). One can never fully eliminate the probability of failure, so high-risk areas often integrate redundancies, carrying excessive resources to maintain minimal functionality (*3*–*5*). Because the possibility of failure is inevitable, recent advances have enabled components to restore functionality through damage, including drone wings repairing midflight (*6*) and both soft actuators and sensors self-healing (*7*, *8*). Classical approaches to failure include algorithmic resiliency and hardware redundancy (*9*).

Although fixed-shape robots optimally execute small sets of known tasks, operating beyond their base functionality requires additional components (*10*). Growing the task space scales the number of integrated functions, which increases the number of compromises in design (*11*). It is therefore difficult to improve adaptability without compromising the failure rate (*12*).

In biology, failure is often overcome through multiagent cooperation (*13*, *14*). Individuals rely on local interactions to overcome their own failures in energy, communication, and sensing (Fig. 1A). Cells passively transport molecules between membranes, making the organism resilient when any single cell dies (*15*–*17*). Mycorrhizal networks share water, nutrients, and communication signals (*18*), whereas acacia trees warn neighbors through airborne signals, resulting in the plant collective being more resilient to single-plant damage or senescence (*19*, *20*). Zooids are animal colonies that share nutrients and physical connections to survive (*21*). Birds share local sensing information through flocking behavior, which is predicted to increase survival rates (*22*–*24*). Ants regulate nutrition on the basis of availability and share pheromone signals when scavenging, ensuring that the path to a food source is maintained even in the event of one or several ants dying (*25*, *26*). Resource sharing, interaction, and cooperation at the cellular level form the very basis for multicellular organisms (*27*).

Separating a robot into individual agents has been shown to improve adaptability to changes in the environment or task (*28*–*30*). Modular robots (MRs) consist of individual agents, called modules, which, when interconnected, form a complete system. These robots are highly adaptive, capable of transforming their shape midoperation to navigate new surroundings (*31*), reaching constricted areas (*32*), and performing fundamentally different tasks, from manipulation to locomotion (*33*–*35*). MRs have potential for applications in challenging environments, such as heavy radiation (*36*), natural disasters (*32*), and space (*37*).

A high number of modules permits more complex shapes, allowing MRs to adapt to a larger set of tasks, but reduces the reliability of the overall system (*38*). A module failing disables some, if not all, of the robot's functionality (*28*), often leading to mission failures (*32*). Past works addressed algorithms such that the robot can simply reconfigure to adapt around failed modules (*39*–*41*) or advised to avoid high numbers of modules to assure reliability (*29*). Proposed methods for adaptation around failed modules include replacing broken modules with functional ones via self-reconfiguration (*42*), designing a robot capable of ejecting failed components and continuing to operate because of built-in redundancy (*43*), or simply continuing to exploit the failed modules as a useful but passive structure that new modules can attach to for entering the operation environment (*36*, *44*). Yet, none of these works has looked into local resource-sharing methodology that would allow to fully restore broken module functionality.

Adding modules generally increases the number of usable components throughout the entire robot. Resource sharing takes embedded components and distributes them across the system to make them hyperredundant. Previous methods for transferring power locally require centralized knowledge of the system topology and active control (*45*, *46*). Communication is fundamental to robots' abilities to respond to instructions but congests with large numbers of modules (*47*–*50*). Fusing sensing among robotic swarms combines the perspectives of individual swarm agents (*51*, *52*) to provide cohesion in flocking (*53*) and robustness to occlusions (*54*). However, fusing all agents into a single filter scales processing and memory needs with the number of sensors. As the MR topology changes, it is difficult to incorporate the necessary physical relationships between sensors. We propose an innovative methodology for sharing critical resources (power, communication, and sensing) without changing the general physical structure of the robot. We implemented this methodology with passive distributed power sharing, hybrid local wireless communication, and a distributed sensor fusion algorithm.

[1]Reconfigurable Robotics Lab, Ecole Polytechnique Fédérale de Lausanne (EPFL), Lausanne, Switzerland. [2]Laboratory of Sustainability Robotics, EPFL, and Swiss Federal Laboratories for Materials Science and Technology (Empa), Lausanne, Switzerland. [3]Laboratory for Analysis and Architecture of Systems (LAAS), CNRS, Toulouse, France.
*Corresponding author. Email: jamie.paik@epfl.ch

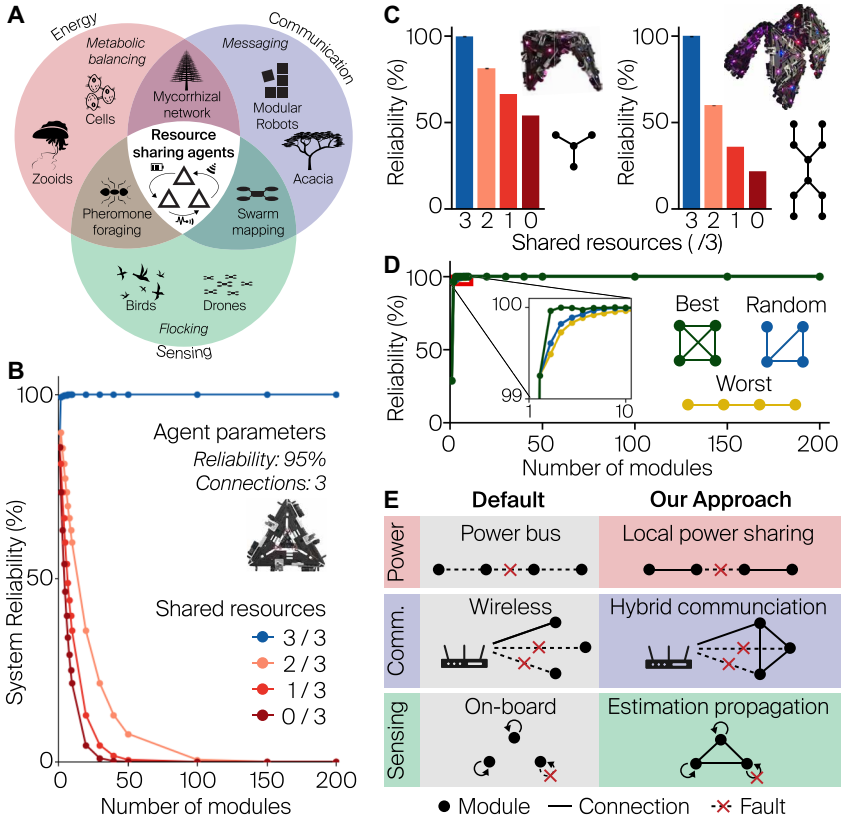

Fig. 1. Local resource sharing among collaborative agents minimizes the effect of individual failures on the overall system. (**A**) Natural and artificial colonies create resilience through sharing energy, communication, and sensing. We integrate critical resource sharing into modular robotics. (**B**) Sharing resources increases system reliability as the number of agents grows. For independent agents, the odds of failure in a system increases with the number of agents. If two of three resources are shared, the reliability decreases. This trend is reversed by sharing all three critical resources. This calculation assumes 95% agent reliability, with each module able to connect up to three others. This was generated via the random topology demonstrated in (D). (**C**) Effects of resource sharing on individual topologies, demonstrated on two different configurations. (**D**) The best-case and worst-case topologies for resource sharing, along with the random topologies in (B). The best case is a fully connected topology, whereas the worst case is a minimally connected line. (**E**) Methods for power, communication, and sensor sharing. Resource-sharing methods for each resource focus on local interactions between agents, preventing a single point of failure.

Sharing one or two resources is not enough (Fig. 1B); if each resource has an equal chance of failure, the system reliability will continue to drop with an increase in number of agents. However, we demonstrate that this trend is reversed when sharing all resources. We applied this approach to individual configurations (Fig. 1C) and provide best- and worst-case failure rates (Fig. 1D). Here, we define "system reliability" as the probability that a robot collective successfully completes a mission, which would otherwise not be possible because of failures of critical resources at the individual-agent level.

We introduce local resource sharing as a paradigm in robotics, reducing the failure rate with an increased number of modules. Sharing resources locally is critical, given that module failures occur with the frequency of a distributed system but have the severity of a centralized system. Centralized methods have a single point of failure and are subject to bottlenecks when scaling in number. A failure in an electrical bus, a wireless interruption, or onboard sensing leaves agents disabled (Fig. 1E). Neighboring modules (connected agents) can compensate for electrical, communication, and sensing failures when there is a single local connection between them. Although vastly different domains, these resources follow the same methodology for sharing in terms of transfer, oscillation prevention, bottlenecks, and propagation, all of which influence the overall system. Through local resource sharing, both reliability and adaptability are improved, fostering sustainability in robotics. Here, we reverse failure trends in robot collectives via a unified model that capitalizes on hyperredundancies among agents across three critical resources—energy, communication, and sensing—the lack of which would otherwise cripple a system. Following this unified model, we show a detailed design, characterization, and validation of resource-sharing methods, including a power-over-communication circuit, a hybrid communication algorithm, and a distributed sensor fusion algorithm, all integrated into a modular robotic system. We demonstrate a robot collective with a multilocomotion scenario operating with full functionality despite one agent having failed, maintaining its functionality through our proposed local resource-sharing methods.

RESULTS

Holistic design and evaluation method for local sharing of critical resources

Although sharing resources improves reliability with the number of agents (Fig. 1B), this trend changes depending on how the modules interconnect (Fig. 1D). We have developed a methodology to model the effect of topology on local resource sharing, shown in Fig. 2. Through this, we are able to assess individual topologies (Fig. 1C), the best- and worse-case scenarios (Fig. 1D), and estimated reliability given a number of modules based on random configurations.

We treat each resource as decoupled and critical; if one fails, the entire system will fail. The probability of a successful mission (e.g., no resource failing) of the collective of agents is the combined probability of each resource not failing throughout the mission

$$p_{\text{success}} = p_{\text{success}}\,(\text{eng})\; p_{\text{success}}(\text{com})\; p_{\text{success}}\,(\text{sen}) \qquad (1)$$

where eng, com, and sen refer to energy, communication, and sensing, respectively. Without resource sharing, each agent is independent, and therefore the probability of a mission succeeding is dictated by the binomial distribution (*29*)

$$p_{\text{success}}(\text{res}) = \left[1 - p_{\text{fail}}(\text{res})\right]^{n_{\text{agents}}} \qquad (2)$$

where $p_{\text{success}}(\text{res})$ is the probability of a resource not failing across the complete system, $p_{\text{fail}}(\text{res})$ is the probability of a resource failing in an agent, and n_{agents} is the number of the system agents.

Individual module failures can be compensated for, depending on their location in an interconnected topology, as shown in Fig. 2A. We define a system failure with resource sharing as a situation where a failed module is only connected to failed neighbors and thus is

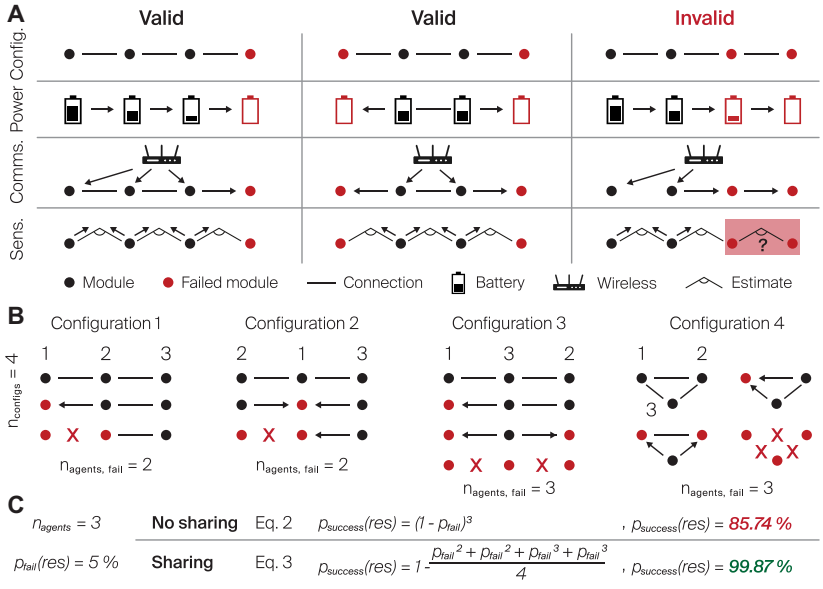

Fig. 2. Effect of topology on resource sharing and mission success. (**A**) How different topologies affect resource sharing. Power and communication are routed from functional to failing modules. If a failed module is only connected to other failed modules, then the angle cannot be accounted for and the system fails. Using this definition of failure mode, (**B**) shows how system reliability is calculated, graphically. For a given number of modules, all possible permutations are defined. Three modules can form either a line or a triangle. All possible combinations of module failures are labeled, and the smallest number of module failures required to determine if the overall system $n_{\text{agents, fail}}$ fails is extracted. These values are used in (**C**), where the probability of a mission success increases by 14%, assuming that a resource has a 5% chance of failure during the mission.

completely unsupported. This is a conservative estimate, given that both power and communication can still propagate past two modules. However, each module does not have enough information to estimate the angle between modules, leading to a failure of the entire system.

To determine the chance of success given a specific number of modules, all possible combinations and failure modes were computed. Given a topology, modules were assigned to fail in a specific order, defining one configuration of failure modes and connections, corresponding to one column in Fig. 2B. Agents failed until the minimum number of agent failures required to cause the configuration to break was calculated, $n_{\text{agents, fail}}$. The maximum number of connections a module can make limits the total number of topologies. Given that the Mori3 can connect to three other modules, we set the maximum number of modules to be three for the sake of Fig. 1, although this value can be altered.

To calculate the chance of success for all topologies given n_{agents}, all failure orders were tested until all combinations of module failures were found. This process was repeated for all possible topologies, testing all combinations of potential failure modes. The final probability is given by the following

$$p_{\text{success}}(\text{res}) = 1 - \frac{\sum \left[p_{\text{fail}}(\text{res})\right]^{n_{\text{agents,fail}}}}{n_{\text{configs}}} \quad (3)$$

where $n_{\text{agents, fail}}$ is the number of failed modules required to cause a configuration failure, with n_{configs} representing the total number of configurations of failure orders. This is shown in Fig. 2C for $n_{\text{agents}} = 3$ and assuming each resource has an arbitrary 5% chance to fail. Sharing resources was found to improve the chance of mission success from 85.74 to 99.87%.

The failure rate depends on the topology of the system, with some topologies proving more resilient than others. Figure 1D shows connection graphs of the best- and worst-case scenarios, along with an example of the "random" topologies as defined above in this section. The best-case scenario is when all modules share as many connections as possible. The best-case scenario was calculated by giving all modules the maximum possible number of connections a module can support, not checking whether these connections are physically viable. All failure orders were considered to find the resilience of the topology. The worst-case scenario is the opposite: the topology with the minimum number of connections and thus with the least support from each module. Such topology has the least number of connections between modules: a line.

Despite underlying differences between resources, each has explicit commonalities that must be implemented through our model. We developed a new circuit that transfers energy between electrical communication contacts at low voltage, adding functionality without mechanical changes. Sharing communication as a resource builds on prior work (*55*), where wireless communication messages were routed to modules through their local communication contacts. Here, we demonstrated an algorithm that enables modules to automatically route messages wirelessly through the local network in the event of a failure. Last, we proposed and implemented a sensor fusion algorithm across a modular system, demonstrating how information from a common factor (e.g., gravity) can refine state estimates without increasing algorithmic complexity. The details of the specific implementation of each resource-sharing methodology are discussed in the Supplementary Materials (*56*).

The proposed unified resource-sharing model is illustrated in Fig. 3. The exact procedure outlined by our model is essential for implementing and modeling resource sharing in a multiagent system. Each resource is transferred according to domain-specific requirements. Given that each resource transaction is symmetric, oversharing could cause a positive feedback loop and oscillations. Resources can overwhelm the local connection through bottlenecks, requiring explicit considerations. Each resource propagates throughout the interconnected system, with local influences defined through proportionalities among individual agents.

First, as shown in Fig. 3, power transfer is described in terms of current I and is dictated by the voltage of the higher-powered source V_{in}, the proportional difference in voltage between power sources (e.g., batteries) in connected modules $n\Delta V$, and a normalizing constant c. Given that current transfer is proportional to the voltage difference, oscillations are reduced. The current must be limited to I_{max} to prevent excessive current damaging wires or overcharging batteries. In our implementation, energy propagates through the robot at an empirically measured rate of $1.440\Delta V$.

Wireless communication propagates through the intermodule communication network, resulting in a total latency L that is determined by the microcontroller processing power, P_{mcu}; the number of intermodule transitions, T_{mcu}; and the wireless latency, L_{wi}. Communication paths naturally form a spanning tree, preventing

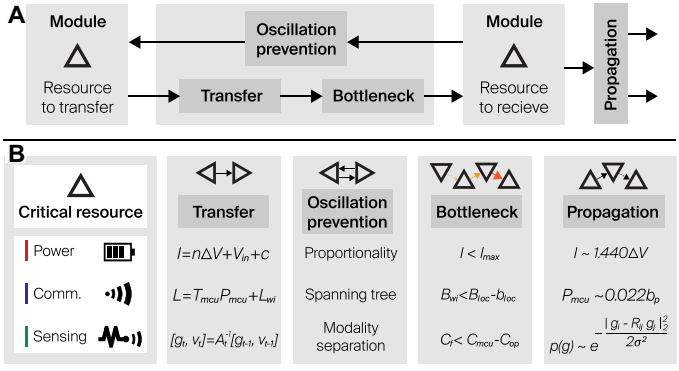

Fig. 3. Model for holistic local sharing across critical resources. The model shows how different resources interplay through local connections and highlights the necessary considerations. (**A**) A general design method for local resource sharing across individual interconnected agents, which must be followed to implement the sharing of critical resources. (**B**) The specific characteristics of each of the three critical resources in the implementation and how they relate to the model. Local sharing of power, wireless communication, and sensing is designed and described through this unified model, despite the fundamental differences in resource type.

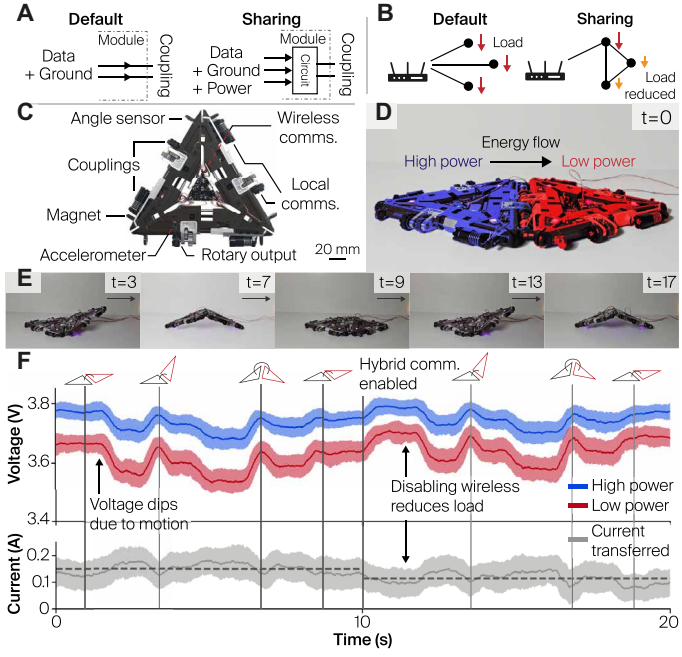

Fig. 4. Power and communication sharing mitigates failure through redundancies and reduces electrical load. (**A** and **B**) Additional functionality gained from resource sharing for power and communication, respectively; circuitry adds power sharing to existing couplings, and disabling wireless communication reduces the power load. (**C**) The MR used in the experiment, Mori3, and its capabilities. (**D**) Power sharing and hybrid communication across two connected modules in motion. Energy is routed from a high-powered module (blue) to a low-powered module (red), which is demonstrated under the extreme case where red has no power source. (**E**) The actuation of the two modules starting from (D). (**F**) The battery voltage in red and blue, with current transfer represented in gray and fluctuating with power load. The dark line and lighter backgrounds, respectively, represent a rolling average and SD of 100 samples (0.4 s). Current transfer was calculated via empirical equations in the model. At 10 s, the red module disabled its wireless communication, remaining functional from support from its neighbor. This action lowered the electrical load, with gray dashed lines showing the average before/after disabling wireless communication and, thus, the lowered current transfer.

oscillations. To avoid overwhelming the local transitions, the data rate from wireless communication, B_{wi}, should be less than the local baud rate, B_{loc}, and the standard communication between modules, b_{loc}. In the case of our Mori3-based validation setup, the latency per module was measured to be 0.022 bytes per ms, b_p (*55*).

Sensor fusion merges sensor data from different modules' sensors by incorporating the transfer of state estimates [g, v] between neighboring modules and local measurements into the precision matrix A, which computes the next time step's estimate, t. Given that estimates are both used and transferred between modules, each modality needs to be separated to prevent ringing. Sensor fusion algorithms can scale in computational complexity of the filter C_f with the number of measurements and must be bound to both the computational power of the microcontroller C_{mcu} and complexity of standard operation C_{op}. By using the transferred neighbors' state estimates to compute the next time step estimates, the sensor information is implicitly propagated throughout the entire connected module network (*57*). The probability $p(g)$ of arriving at a global state of a common factor (e.g., gravity g) for each module is subject to onboard g_i and neighboring unit gravity measurements g_j, which are reoriented relative to a module's reference frame via R_{ij}.

Local resource propagation compensates for power, communication, and sensing failures

We show that through our method, power sharing, hybrid communication, and sensor fusion allow the system to operate despite subcomponent failures. Power and communication are transferred simultaneously between modules through the same local electrical contacts. Although adding power-sharing circuitry, we add functionality without increasing mechanical complexity (Fig. 4A and Materials and Methods). Wireless communication is routed from a central hub through the local messaging network, providing redundancy in the event of a wireless connection failure and reducing power consumption (Fig. 4B and Materials and Methods). This is demonstrated by showing continued operation with one of two modules failed on the Mori3 MR (*34*). Mori3 consists of triangular modules, which are able to rotate around joints coupled to their connected neighbors (Fig. 4C). Each connection has two outgoing electrical pins, used to communicate locally between agents, as well as a wireless connection for Wi-Fi.

In the experimental validation, two Mori3 modules were connected, one with high power and the other with lower power (Fig. 4D and movie S2). As an extreme example, the low-power module operated without both a power source and sensing capabilities. The connected modules alternated between interangles of ±45°, both requiring continuous synchronization (Fig. 4E). The left module routed power to the connected module on the right through the former data lines. Midway through the experiment, wireless communication was disabled on the module on the right, reducing power consumption. This communication failure was detected by a watchdog timer, and the system adapted to route wireless information through the local network. Communication remained fully operational; instructions were routed from the left module to its neighbor, and ongoing messages between modules synchronized motion. The two modules remained fully functional despite one module having three critical failures. The battery voltages of both modules are shown in Fig. 4F, with current transfer between them calculated via empirical measurements and the

model. After disabling wireless communication, the average current dropped by around 36 mA. This is consistent with the measured wireless current draw of the Mori3 system of 37 mA (*55*). Throughout the experiment, sensor values were constantly exchanged, with the local sensor fusion algorithm compensating for the failed sensing of the left module.

We demonstrate an onboard sensor fusion algorithm that exploits local intermodule correlations to obtain a robust state estimation. Modules combined both local and neighboring state estimates and measurements, still estimating their own state even with all onboard sensors disabled. The sensor fusion algorithm consists of two congruently operating components: one that estimates the angle between modules and another that estimates the direction of gravity as a common factor. Information about the common factor propagated through connected modules to the whole system (Fig. 5A). This algorithm runs on embedded processors with low computational power, unaffected by the number of modules or interconnected topology.

As a test platform, Mori3 can use three different types of measurement for the intermodule angle. Mori3 has rotary Hall effect sensors, which give the absolute angle between two modules (*34*). Given that the couplings are symmetric, neighboring modules also contain Hall effect sensors measuring the same angle, which are exchanged between modules. An accelerometer measures the gravity vector, determining the plane of Mori3's orientation. The relative orientations of a module and neighbor can calculate the relative angle between face planes, adding a tertiary method of measuring the rotary joint. The gravity measurement is a common factor among all modules; through propagating gravity estimates, each module achieves a more accurate estimate of the angle between agents.

In the experimental validation of the sensor fusion, Mori3 was connected as an arm consisting of three modules, adding modules until a closed chain of six was formed (Fig. 5B). Our local resource-sharing sensor fusion algorithm substantially improved the accuracy of the module's angle estimate compared with the raw sensor values (Fig. 5, C and D). If a module's sensing capabilities were disabled, not only did the system continue to function but also there was no negative effect on the system. Sensor fusion notably reduced error in the event of a closed chain; the algorithm ensures that all modules have a similar approximation of a common factor, gravity, thus overcoming sensor biases induced by additional forces that misalign axes.

We demonstrate a robot collective operating with a module missing three critical resources. Figure 6 shows a set of four Mori3 modules connected into a tripod structure performing a locomotion task in a challenging environment (movie S1). The central module of the tripod had no battery, and its sensing and wireless capabilities were disabled. This module was effectively "dead" and thus completely reliant on its neighbors for resources to allow the overall system to successfully locomote. All coupled joints need to be actively controlled by each individual module synchronously with the coupled neighbor. Otherwise, if one was actively moving and the other passive and stuck, the joint could tear itself apart. If the central module remained defunct, then any actuation between modules would result in errors or break the system.

Figure 6 (A to C) shows normal operation without sharing any resources. Without sharing resources, the collective could not share power with the central module or exchange sensor information or other messages with it to coordinate the join motions. Therefore, the central disabled agent could not move its legs, and active agents could only spin their integrated wheels from the outer edges, effectively driving on the ground. The collective could only drive slowly and ceased operation after a module lost power and continuously restarted. Such locomotion is slower and draws more power; the modules ran out of charge at 809 s of continuous operation, and the collective failed to pass under the overpass.

To locomote via walking, all four modules are necessary; a single failure would break the system, with the central module being the most critical. Through our proposed methodology, neighboring modules bring the central dead module back to life by sharing all critical resources: power, sensing, and wireless communication. Figure 6 (D to F) showcases different locomotion techniques integrated into Mori3 that adapt to the environment: walking and driving. The overhead path is shown in the center of Fig. 6, with motion shown along the outside. The tripod structure walked toward a bridge (t_0 to t_3; 0 to 182 s), flattened under the bridge, and then

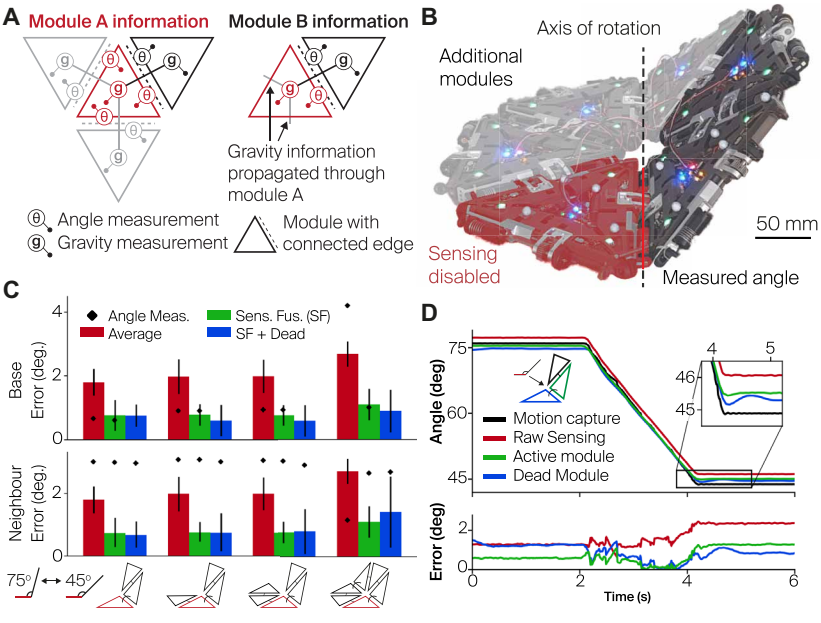

Fig. 5. Local sensor fusion improves sensing and allows the system to operate despite subcomponent failure. (**A**) The information available to each module, where information refers to knowledge about a global state: both estimates and measurement data. Module A (red) has all information from its surrounding neighbors. Module B has only module A connected to it but receives information implicitly from module A's neighbors through module A's estimate. (**B**) The characterization setup, with results in (**C**). The graphs show the absolute mean error and SD between the base module and its neighbor's estimate and motion capture data. Each bar corresponds to one experimental run per sensing method. The individual angle sensor measurements from each module are shown as diamonds. Three connected modules were alternating between 75° and 45° angles, controlled by the average of angle sensor data between two modules (red), sensor fusion (green), or sensor fusion with all sensors disabled on the bottom module (blue). This process was repeated with additional modules along the base. Sensor fusion substantially improved angle estimates relative to raw sensor data, and the presence of a dead module had only a minor effect on the estimates of each module. (**D**) A sample of the raw, fused, and dead estimate data (fused data come from the neighbor; active module, green).

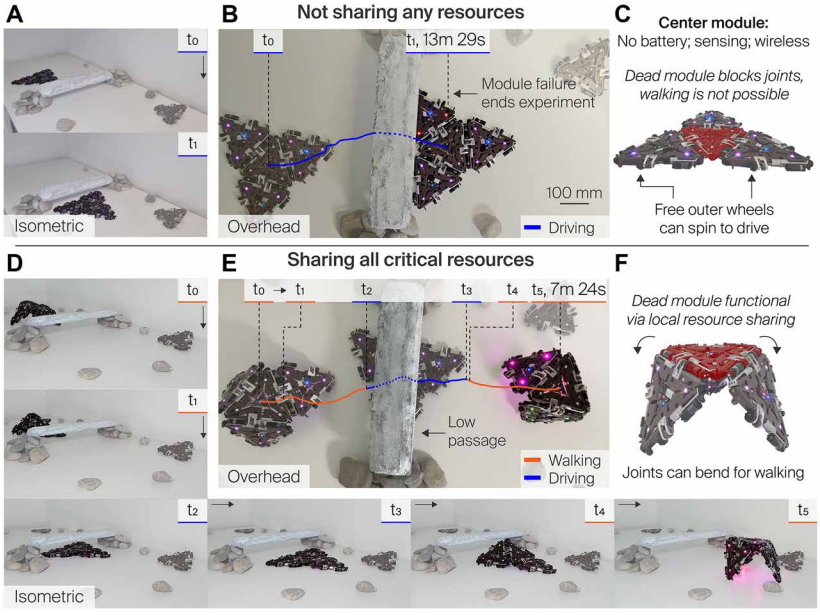

Fig. 6. Four connected modules locomoting with a completely defunct module. Two experiments were performed; without (**A** to **C**) and with (**D** to **F**) resource sharing. (B) and (E) show an overhead view, with motion from left to right. The surrounding images, (A) and (D), show experiment progression at specific time points (t_x), arranged sequentially in a counterclockwise direction. The structure of the system is shown in (C) and (F), with the central agent marked in red without battery, wireless communication, or sensing capabilities. (A) to (C) show the collective operating without local resource sharing and failing to complete the locomotion mission at t_1 time point because of one of the modules running out of power, whereas (D) to (F) show it operating with local resource sharing. Sharing enables both forms of locomotion, reenabling alternate and more efficient methods of motion, such as walking, allowing the robot to complete its mission.

used wheels integrated into Mori3's couplings to drive below the bridge (t_3 to t_4; 182 to 330 s). Once the bridge was passed, the tripod rose and continued to walk until it reached its target location (t_5 to t_7; 330 to 444 s).

Through sharing, the resources missing in the central module were completely compensated by its neighbors. This shows a notable and contradictory result: An agent was effectively dead through lack of resources but continued operating with its full capacity.

DISCUSSION

We proposed and validated a method to capitalize on hyperredundancies to reverse failure likelihood trends in multiagent systems via local resource sharing. We demonstrated sharing in three critical resources: power, communication, and sensing. Paradoxically, a robot was demonstrated to successfully function with a complete subsystem failure; one module had no functioning power, communication, or sensing but was supported through its neighbors. We presented a holistic model for sharing fundamentally different resources and its effects across different interconnected topologies. We validated the presented model with two modules maintaining functionality and only one having critical resources and characterized the sensor fusion's accuracy with a sensing failure.

This method applies to failures of local resources and assumes that modules are not destroyed, maintaining some degree of subsystem autonomy. If a module is destroyed, then it simply cannot benefit from local resource sharing but can still serve as a passive component in the structure (*36*, *44*). However, we argue that the definition of a failure also encapsulates component and subsequent resource failures, which was solved through our work. Although we do not encompass all definitions of failures, we still showed a robotic system with resource-failed agents performing at full functional capacity. Subsequently, a connection failure between modules can also be approximated as a module itself failing. This approximation will lead to an even more conservative estimate of the probability of success according to the topology model, given that although the local sharing method might have failed, the resource still exists in the module and can continue to function.

To generalize this approach to other robot collectives, this work requires an electrical connection, local communication, and/or a common sensing factor between modules. Without an electrical connection, power cannot be shared. In this work, communication was done via electrical contacts, with power routed over these communication lines. Our method can still apply to modules with other methods of communication, such as infrared, allowing for local sharing of communication and sensing. For local sharing, each module needs to have a common shared factor, which was gravity in this work. Any other common factors, such as pressure, solar input, magnetic orientation, or even time, can be propagated to improve the accuracy of the system's state estimate.

Our approach provides a mathematical and physical basis for studying how resource sharing influences the survival chances of a system, organism, or society. Future work can test different characteristics of biological swarms on physical robots, furthering our understanding of both natural and artificial colonies. In a robotic swarm, the behavior of the collective is a direct result of local interactions between agents (*58*). In our work, we study the methodology of resource sharing that arises from local interactions between robots in a MR collective. The same ideas and concepts can extend to swarms with hardware adaptations that allow swarm members to dock to each other for energy and information transfer. Furthermore, future work could focus on extending our proposed resource-sharing methodology by incorporating additional types of resources that might need to be shared in a swarm, such as local path plans or local behavior parameters (*54*, *59*), which would further enhance the resilience of a robotic swarm to an individual agent's failures.

Future work will also explore scaling the number of agents in the system. Although this study focused on minimal configurations, where each agent plays a critical role and failures have substantial consequences, the insights gained provide a strong foundation for understanding behavior in larger collectives. In systems with many modules, the failure of a single agent may have limited effects on the overall system, but the principles of resource sharing and fault tolerance established here will remain applicable. Adding local resource-sharing methods adds complexity through additional components and algorithms, which themselves can fail. This leads to questions pertaining to what extent modular systems and swarms should focus on agent survival versus system-level reconfiguration to mitigate the effects of failures and how many agents in a collective should be involved in these efforts.

Ultimately, reliability-related challenges have prevented MRs from being used in practical applications. Through local resource sharing, we are able to improve MR system reliability with an increased number of modules. The findings of this work demonstrate the potential of highly adaptive robots to operate through otherwise critical failures, resolving the conflict between adaptability and reliability.

MATERIALS AND METHODS

Model implementation of local power sharing

Power sharing combines redundant power sources into a single system through the electrical couplings between modules. Our methodology combines electrical functionality without adding mechanical complexity. The developed method balances batteries between modules without active control, with safeguards preventing large currents. The power sharing uses the following model, as described in Fig. 4A, and is defined by

$$I = n\Delta V + V_{\text{in}} + c \tag{4}$$

where I is the current transferred between modules, ΔV is the difference in voltage between modules, V_{in} is the higher-powered voltage source (the higher voltage of the two modules), and n and c are empirically determined constants. Given that a battery's voltage decreases with lower state of charge, power naturally propagates from modules with more power to those with less. Because the transfer is proportional to ΔV, transfer is reduced when approaching equal energy charges between modules, thereby preventing oscillations.

Determined empirically (measurements shown in fig. S1E), current transfer is defined by

$$I \propto 1.440\Delta V \tag{5}$$

which can be used in conjunction with battery models to accurately model the response of diverse topologies (*60*). Note that if ΔV is 0, then the circuit still draws some quiescent power, particularly depending on the amount of data being transferred between agents, which does not dictate the amount of power that propagates through the overall modular network, thus excluding the V_{in} and c terms from Eq. 4.

The amount of current transferred has to be limited to avoid burning out electrical contacts (*61*), as well as not to overcharge batteries, causing damage. The bottleneck for power transfer is dictated by current without other factors and is defined by

$$I < I_{\text{max}} \tag{6}$$

where I_{max} is the maximum allowable current between modules. In our implementation, I_{max} is set to $0.5A$ to stay within the battery's acceptable charging rates.

Model implementation of hybrid communication

Hybrid communication routes wireless traffic through intermodule local messages, ensuring that disabling the wireless functionality of a single module does not cause system failure. Communication distribution integrates classical networking techniques to improve robustness without overloading local communications. Routing through the local network introduces latency according to the capacity of intermodule communication

$$^{L=T}\text{mcu}^{P}\text{mcu}^{+L}\text{wi} \tag{7}$$

where L is the total latency of a message passing through a module, T_{mcu} is the number of intermodule transitions to send the message, P_{mcu} is the microcontroller processing power (i.e., the processing time it takes for a microcontroller to process a message), and L_{wi} is the wireless latency. Messages default to a spanning tree, preventing oscillations. Between agents, the additional processing time is characterized empirically by

$$P_{\text{mcu}} \propto 0.022b_{\text{p}} \tag{8}$$

where b_{p} is the message size and 0.022 is processing time in milliseconds. To prevent overloading the local communication, messages to and from wireless to a module, B_{wi}, should be capped by both the local baud rate, B_{loc}, and any continuous synchronizing communication between modules, B_{loc}.

$$B_{\text{wi}} < B_{\text{loc}} - b_{\text{loc}} \tag{9}$$

In our implementation, B_{loc} is limited by the local baud rate between agents of 460,800 bits per second (bps), with B_{loc} at ~500 bps during standard operation.

Model implementation of local sensor fusion with estimation propagation

Sensor fusion integrates estimates from neighboring modules to refine a module's state estimate. Estimates of a module's local state, v, and the common factor, gravity g, are propagated as follows

$$[g_t, v_t] = A_t^{-1}\,[g_{t-1}, v_{t-1} \tag{10}$$

where A is the precision matrix and v is the information vector. Modality separation decouples interactions between filters to minimize their mutual effects and prevent oscillations.

Propagation of information across distributed systems is defined by

$$p(g) \propto e^{-\frac{|g_i - R_{ij}g_j|_2^2}{2\sigma^2}} \tag{11}$$

where $p(g)$ is the probability of arriving to the global state of a common factor g for each module. This equation is inspired by an energy-based model for factor graphs in the context of Gaussian belief propagation (*57*). $p()$ represents a single multivariate Gaussian distribution, containing all Gaussian factors in the whole sensor fusion framework across the modules. Because energy in this model is additive, this distribution contains all information and, therefore, the influence of each sensor. Probabilities are influenced by local and neighboring measurements, g_i and g_j, and are reoriented about a module's reference frame via R_{ij}.

Filter complexity scales with the number of sensor inputs, which can overload a module's computational capacity

$$C_{\text{f}} < C_{\text{mcu}} - C_{\text{op}} \tag{12}$$

where C_{f}, C_{mcu}, and C_{op} are the computational capacity of the filter, the capacity of the microcontroller, and the used capacity from normal operation. Our filter can estimate the angle of three edges and gravity with onboard embedded processors (74 MHz) on top of existing robot operations.

Supplementary Materials

The PDF file includes:

Materials and Methods
Figs. S1 to S4
Legends for movies S1 to S3
References (*62*–*64*)

Other Supplementary Material for this manuscript includes the following:
Movies S1 to S3

REFERENCES AND NOTES

1. A. F. Winfield, J. Nembrini, Safety in numbers: Fault-tolerance in robot swarms. *Int. J. Model. Identif. Control* **1**, 30–37 (2006).
2. G.-Z. Yang, J. Bellingham, P. E. Dupont, P. Fischer, L. Floridi, R. Full, N. Jacobstein, V. Kumar, M. McNutt, R. Merrifield, B. J. Nelson, B. Scassellati, M. Taddeo, R. Taylor, M. Veloso, Z. L. Wang, R. Wood, The grand challenges of *Science Robotics*. *Sci. Robot.* **3**, eaar7650 (2018).
3. R. Thandiackal, K. Melo, L. Paez, J. Herault, T. Kano, K. Akiyama, F. Boyer, D. Ryczko, A. Ishiguro, A. J. Ijspeert, Emergence of robust self-organized undulatory swimming based on local hydrodynamic force sensing. *Sci. Robot.* **6**, eabf6354 (2021).
4. G. Brantner, O. Khatib, Controlling Ocean One: Human–robot collaboration for deep-sea manipulation. *J. Field Robot.* **38**, 28–51 (2021).
5. Boeing Corporation Aerospace Group, "Integrated manned interplanetary spacecraft concept definition" (tech. rep. NASA-CR-6658, National Aeronautics and Space Administration, 1968).
6. S. Kim, Y. H. Hsiao, Y. Lee, W. Zhu, Z. Ren, F. Niroui, Y. Chen, Laser-assisted failure recovery for dielectric elastomer actuators in aerial robots. *Sci. Robot.* **8**, eadf4278 (2023).
7. H. Bai, Y. S. Kim, R. F. Shepherd, Autonomous self-healing optical sensors for damage intelligent soft-bodied systems. *Sci. Adv.* **8**, eabq2104 (2022).
8. S. Terryn, J. Brancart, D. Lefeber, G. Van Assche, B. Vanderborght, Self-healing soft pneumatic robots. *Sci. Robot.* **2**, eaan4268 (2017).
9. M. L. Visinsky, J. R. Cavallaro, I. D. Walker, Robotic fault detection and fault tolerance: A survey. *Reliab. Eng. Syst. Safety* **46**, 139–158 (1994).
10. M. E. Sayed, J. O. Roberts, R. McKenzie, S. Aracri, A. Buchoux, A. A. Stokes, Limpet II: A modular, untethered soft robot. *Soft Robot.* **8**, 319–339 (2021).
11. S. Miyashita, S. Guitron, S. Li, D. Rus, Robotic metamorphosis by origami exoskeletons. *Sci. Robot.* **2**, eaao4369 (2017).
12. D. N. Lyttle, J. P. Gill, K. M. Shaw, P. J. Thomas, H. J. Chiel, Robustness, flexibility, and sensitivity in a multifunctional motor control model. *Biol. Cybern.* **111**, 25–47 (2017).
13. J. A. Ågren, N. G. Davies, K. R. Foster, Enforcement is central to the evolution of cooperation. *Nat. Ecol. Evol.* **3**, 1018–1029 (2019).
14. J. Gross, Z. Z. Méder, C. K. W. de Dreu, A. Romano, W. E. Molenmaker, L. C. Hoenig, The evolution of universal cooperation. *Sci. Adv.* **9**, eadd8289 (2023).
15. S. Son, M. M. Stevens, H. X. Chao, C. Thoreen, A. M. Hosios, L. D. Schweitzer, Y. Weng, K. Wood, D. Sabatini, M. G. Vander Heiden, S. Manalis, Cooperative nutrient accumulation sustains growth of mammalian cells. *Sci. Rep.* **5**, 17401 (2015).
16. W. Palm, C. B. Thompson, Nutrient acquisition strategies of mammalian cells. *Nature* **546**, 234–242 (2017).
17. M. Zhernenkov, D. Bolmatov, D. Soloviov, K. Zhernenkov, B. P. Toperverg, A. Cunsolo, A. Bosak, Y. Q. Cai, Revealing the mechanism of passive transport in lipid bilayers via phonon-mediated nanometre-scale density fluctuations. *Nat. Commun.* **7**, 11575 (2016).
18. S. W. Simard, K. J. Beiler, M. A. Bingham, J. R. Deslippe, L. J. Philip, F. P. Teste, Mycorrhizal networks: Mechanisms, ecology and modelling. *Fungal Biol. Rev.* **26**, 39–60 (2012).
19. M. Toyota, D. Spencer, S. Sawai-Toyota, W. Jiaqi, T. Zhang, A. J. Koo, G. A. Howe, S. Gilroy, Glutamate triggers long-distance, calcium-based plant defense signaling. *Science* **361**, 1112–1115 (2018).
20. I. T. Baldwin, J. C. Schultz, Rapid changes in tree leaf chemistry induced by damage: Evidence for communication between plants. *Science* **221**, 277–279 (1983).
21. J. S. Ryland, G. F. Warner, Growth and form in modular animals: Ideas on the size and arrangement of zooids. *Philos. Trans. R. Soc. Lond. B Biol. Sci.* **313**, 53–76 (1986).
22. W. A. Thompson, I. Vertinsky, J. R. Krebs, The survival value of flocking in birds: A simulation model. *J. Anim. Ecol.* **43**, 785–820 (1974).
23. M. Jullien, J. Clobert, The survival value of flocking in Neotropical birds: Reality or fiction? *Ecology* **81**, 3416–3430 (2000).
24. G. Beauchamp, Flocking in birds increases annual adult survival in a global analysis. *Oecologia* **197**, 387–394 (2021).
25. A. Dussutour, V. Fourcassié, D. Helbing, J.-L. Deneubourg, Optimal traffic organization in ants under crowded conditions. *Nature* **428**, 70–73 (2004).
26. A. Dussutour, S. J. Simpson, Communal nutrition in ants. *Curr. Biol.* **19**, 740–744 (2009).
27. M. D. Herron, P. L. Conlin, W. C. Ratcliff, *The Evolution of Multicellularity* (CRC Press, 2022).
28. J. Seo, J. Paik, M. Yim, Modular reconfigurable robotics. *Annu. Rev. Control Robot. Auton. Syst.* **2**, 63–88 (2019).
29. K. Støy, "Reconfigurable robots" in *Springer Handbook of Computational Intelligence* (Springer-Verlag, 2015), pp. 1407–1421.
30. T. Chen, X. Yang, B. Zhang, J. Li, J. Pan, Y. Wang, Scale-inspired programmable robotic structures with concurrent shape morphing and stiffness variation. *Sci. Robot.* **9**, eadl0307 (2024).
31. Y. Ozkan-Aydin, D. I. Goldman, Self-reconfigurable multilegged robot swarms collectively accomplish challenging terradynamic tasks. *Sci. Robot.* **6**, eabf1628 (2021).
32. J. Daudelin, G. Jing, T. Tosun, M. Yim, H. Kress-Gazit, M. Campbell, An integrated system for perception-driven autonomy with modular robots. *Sci. Robot.* **3**, eaat4983 (2018).
33. S. Hauser, M. Mutlu, P. A. Léziart, H. Khodr, A. Bernardino, A. J. Ijspeert, Roombots extended: Challenges in the next generation of self-reconfigurable modular robots and their application in adaptive and assistive furniture. *Robot. Auton. Syst.* **127**, 103467 (2020).
34. C. H. Belke, K. Holdcroft, A. Sigrist, J. Paik, Morphological flexibility in robotic systems through physical polygon meshing. *Nat. Mach. Intell.* **5**, 669–675 (2023).
35. C. E. Gregg, D. Catanoso, O. I. B. Formoso, I. Kostitsyna, M. E. Ochalek, T. J. Olatunde, I. W. Park, F. M. Sebastianelli, E. M. Taylor, G. T. Trinh, K. C. Cheung, Ultralight, strong, and self-reprogrammable mechanical metamaterials. *Sci. Robot.* **9**, eadi2746 (2024).
36. M. E. Sayed, J. O. Roberts, K. Donaldson, S. T. Mahon, F. Iqbal, B. Li, S. Franco Aixela, G. Mastorakis, E. T. Jonasson, M. P. Nemitz, S. Bernardini, A. A. Stokes, Modular robots for enabling operations in unstructured extreme environments. *Adv. Intell. Syst.* **4**, 2000227 (2022).
37. V. Zykov, E. Mytilinaios, M. Desnoyer, H. Lipson, Evolved and designed self-reproducing modular robotics. *IEEE Trans. Robot.* **23**, 308–319 (2007).
38. M. Rubenstein, A. Cornejo, R. Nagpal, Programmable self-assembly in a thousand-robot swarm. *Science* **345**, 795–799 (2014).
39. M. Yim, B. Shirmohammadi, J. Sastra, M. Park, M. Dugan, C. J. Taylor, "Towards robotic self-reassembly after explosion" in *IEEE/RSJ International Conference on Intelligent Robots and Systems* (IEEE, 2007), pp. 2767–2772.
40. C. Parrott, T. J. Dodd, R. Groß, "HiGen: A high-speed genderless mechanical connection mechanism with single-sided disconnect for self-reconfigurable modular robots" in *IEEE/RSJ International Conference on Intelligent Robots and Systems* (IEEE, 2014), pp. 3926–3932.
41. C. Liu, M. Yim, "Configuration recognition with distributed information for modular robots" in *Robotics Research: The 18th International Symposium ISRR*, N. M. Amato, G. Hager, S. Thomas, M. Torres-Torriti, Eds. (Springer, 2020), pp. 967–983.
42. A. Spröwitz, R. Moeckel, M. Vespignani, S. Bonardi, A. J. Ijspeert, Roombots: A hardware perspective on 3D self-reconfiguration and locomotion with a homogeneous modular robot. *Robot. Auton. Syst.* **62**, 1016–1033 (2014).
43. T. Cordie, J. Roberts, M. Dunbabin, R. Dungavell, T. Bandyopadhyay, Enabling robustness to failure with modular field robots. *Front. Robot. AI* **11**, 1225297 (2024).
44. S. Li, R. Batra, D. Brown, H. D. Chang, N. Ranganathan, C. Hoberman, D. Rus, H. Lipson, Particle robotics based on statistical mechanics of loosely coupled components. *Nature* **567**, 361–365 (2019).
45. G. Liang, Y. Tu, L. Zong, J. Chen, T. L. Lam, "Energy sharing mechanism for a freeform robotic system-FreeBOT" in *2022 International Conference on Robotics and Automation (ICRA)* (IEEE, 2022), pp. 4232–4238.
46. H. Arai, N. Satoh, "A power sharing modular robot with power packet technology" in *2021 23rd European Conference on Power Electronics and Applications* (IEEE, 2021), pp. 1–6.
47. R. F. M. Garcia, K. Stoy, D. J. Christensen, A. Lyder, "A self-reconfigurable communication network for modular robots" in *Proceedings of the International Conference on Robot Communication and Coordination* (ICST, 2007).
48. J. Baca, B. Woosley, P. Dasgupta, C. A. Nelson, Configuration discovery of modular self-reconfigurable robots: Real-time, distributed, IR+ XBee communication method. *Robot. Auton. Syst.* **91**, 284–298 (2017).
49. A. Ghaffari, Congestion control mechanisms in wireless sensor networks: A survey. *J. Netw. Comput. Appl.* **52**, 101–115 (2015).
50. M. S. Talamali, A. Saha, J. A. Marshall, A. Reina, When less is more: Robot swarms adapt better to changes with constrained communication. *Sci. Robot.* **6**, eabf1416 (2021).
51. S. Lynen, M. W. Achtelik, S. Weiss, M. Chli, R. Siegwart, "A robust and modular multi-sensor fusion approach applied to mav navigation" in *IEEE/RSJ International Conference on Intelligent Robots and Systems* (IEEE, 2013), pp. 3923–3929.
52. K. H. Petersen, N. Napp, R. Stuart-Smith, D. Rus, M. Kovac, A review of collective robotic construction. *Sci. Robot.* **4**, eaau8479 (2019).
53. E. Soria, F. Schiano, D. Floreano, Predictive control of aerial swarms in cluttered environments. *Nat. Mach. Intell.* **3**, 545–554 (2021).
54. X. Zhou, X. Wen, Z. Wang, Y. Gao, H. Li, Q. Wang, T. Yang, H. Lu, Y. Cao, C. Xu, F. Gao, Swarm of micro flying robots in the wild. *Sci. Robot.* **7**, eabm5954 (2022).
55. K. A. Holdcroft, C. H. Belke, A. Sigrist, S. Bennani, J. Paik, Hybrid wireless–local communication via information propagation for modular robotic synchronization applications. *Adv. Intell. Syst.* **4**, 2100226 (2022).
56. Materials and methods are available as the Supplementary Materials.
57. J. Ortiz, T. Evans, A. J. Davison, A visual introduction to Gaussian belief propagation. arXiv:2107.02308 [cs.AI] (2021).
58. M. Y. Ben Zion, J. Fersula, N. Bredeche, O. Dauchot, Morphological computation and decentralized learning in a swarm of sterically interacting robots. *Sci. Robot.* **8**, eabo6140 (2023).
59. E. R. Magsino, F. A. V. Beltran, H. A. P. Cruzat, G. N. M. De Sagun, "Simulation of search-and-rescue and target surrounding algorithm techniques using Kilobots" in *2016 2nd International Conference on Control, Automation and Robotics (ICCAR)* (IEEE, 2016), pp. 70–74.

60. K. A. Holdcroft, C. H. Belke, S. Bennani, J. Paik, 3PAC: A plug-and-play system for distributed power sharing and communication in modular robots. *IEEE/ASME Trans. Mechatron.* **27**, 858–867 (2021).
61. M. H. Yim, "Constant current power supply system for connectable modular elements," US Patent 6,150,738 (2000).
62. C. E. Rasmussen, C. K. Williams, *Gaussian Processes for Machine Learning* (MIT Press, 2006).
63. Oxford English Dictionary, "resource, n" (Oxford Univ. Press, 2010), https://oed.com/dictionary/resource_n.
64. A. Bolotnikova, K. Holdcroft, H. Cerbone, C. Belke, A. Ijspeert, J. Paik, Optimized user-guided motion control of modular robots. *Nat. Commun.* **16**, 8675 (2025).

Acknowledgments: We thank E. Roy for meticulous work in maintaining the hardware of Mori3; C. Stocker, D. Cisier, and H. Cerbone for initial explorations into sensor fusion; A. Schüssler and S. Demirtas for assistance during experimental sessions; and A. Sigrist for helpful discussions. **Funding:** This research was supported in part by the EPFL Center for Intelligent Systems (CIS), the European Space Agency's (ESA) Networking/Partnering Initiative (NPI 646-2018), Swiss Space Innovation, and the Swiss National Centre of Competence in Research (NCCR) in Robotics. **Author contributions:** Conceptualization: K.H. and J.P. Funding acquisition: J.P. Investigation: K.H. and A.B. Methodology: K.H., A.B., and A.J.M. Software: K.H., A.B., and A.J.M. Supervision: J.P. Visualization: K.H. and A.B. Writing—original draft: K.H., A.B., and A.J.M. Writing—review and editing: K.H., A.B., and J.P. **Competing interests:** The authors declare that they have no competing interests. **Data, code, and materials availability:** All code is available online at the following DOI: 10.5281/zenodo.18189133. The manuscript otherwise contains all information to recreate this work. Experiments were performed on the Mori3 MR (*34*). All other materials, electronics, and hardware used in this work are commercially available.

Submitted 29 April 2025
Accepted 15 January 2026
Published 11 February 2026
10.1126/scirobotics.ady6304

Science Robotics

Scalable robot collective resilience by sharing resources

Kevin Holdcroft, Anastasia Bolotnikova, Antoni Jubés Monforte, and Jamie Paik

Sci. Robot. **11** (111), eady6304. DOI: 10.1126/scirobotics.ady6304

Science Robotics (ISSN 2470-9476) is published by the American Association for the Advancement of Science. 1200 New York Avenue NW, Washington, DC 20005. The title *Science Robotics* is a registered trademark of AAAS.